Vibrational Study of Organometallic Complexes with Thiophene Ligands: Models for Adsorbed Thiophene on Hydrodesulfurization Catalysts

Patrick Mills, Scott Korlann, and Mark E. Bussell*

Department of Chemistry, MS-9150, Western Washington University, Bellingham, Washington 98225

Michael A. Reynolds, Maxim V. Ovchinnikov, and Robert J. Angelici

Ames Laboratory and Department of Chemistry, Iowa State University, Ames, Iowa 50011

Christoph Stinner, Thomas Weber, and Roel Prins

Laboratorium für Technische Chemie, ETH-Zentrum, CH-8092 Zürich, Switzerland

Received: January 22, 2001

Interpretation and comparison of the vibrational spectra of organometallic complexes containing thiophene ligands with IR spectra of adsorbed thiophene on sulfided Mo/Al_2O_3 catalysts have permitted a definitive assignment of the adsorption mode of the surface-bonded thiophene. Infrared and Raman spectra were acquired for three organometallic complexes: (η^5-C_5D_5)$Re(CO)_2$(η^1(S)-C_4H_4S), (η^5-C_4H_4S)$Cr(CO)_3$, and [(η^5-C_4H_4S)-$Mn(CO)_3$]BF_4. The vibrational properties of η^1(S)- and η^5-coordinated thiophene were further investigated through normal-mode analyses of the IR spectra of thiophene coordinated in (η^5-C_4H_4S)$Cr(CO)_3$ and (η^5-C_5D_5)$Re(CO)_2$(η^1(S)-C_4H_4S). Perturbations among the force constants of a gas-phase thiophene model, consistent with the structure of η^1(S)- and η^5-coordinated thiophene ligands, gave rise to respective thiophene force fields that allowed for the accurate determination of the IR spectra of thiophene coordinated in the Cr and Re complexes. Spectral shifts observed for the IR spectrum of the η^1(S)-coordinated thiophene ligand, with respect to the IR spectrum of free thiophene, are similar to those observed for analogous bands of thiophene adsorbed at the surface of sulfided Mo/Al_2O_3 catalysts. Furthermore, perturbations among the force constants of η^1(S)-coordinated thiophene, necessary to model such shifts, indicate that the hydrocarbon backbone of thiophene is strengthened upon η^1(S) adsorption, whereas the C−S bonds are significantly weakened. These bonding changes, along with the assignment of the adsorption mode of thiophene, suggest an HDS mechanism in which the initial steps are η^1(S) adsorption of thiophene followed by subsequent cleavage of one of the C−S bonds.

Introduction

Thiophene (C_4H_4S) is often used as a model organosulfur compound for research investigations of the hydrodesulfurization (HDS) process.[1,2]

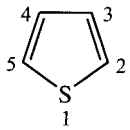

Despite years of research, there is no consensus on the elementary HDS reaction steps whereby sulfur is selectively removed from thiophene adsorbed on a catalyst surface. In the industrial process, hydrodesulfurization of organosulfur compounds in fossil fuels is carried out over alumina-supported molybdenum or tungsten catalysts promoted with cobalt or nickel (e.g., $Co-Mo/Al_2O_3$).[2] The catalysts are sulfided prior to use and evidence suggests that the active catalytic phase consists of MoS_2-like structures with Co atoms located at their edges. The active sites for the HDS reaction are also believed to be located on the edge planes of the highly anisotropic MoS_2-like structures where sulfur vacancies expose coordinately unsaturated (cus) Mo sites.[2]

Two recent studies have utilized vibrational spectroscopic techniques to investigate the adsorption of thiophene on alumina-supported, sulfided molybdenum catalysts (Mo/Al_2O_3). Mitchell et al.[3] utilized inelastic neutron scattering (INS) to investigate the vibrational spectrum of adsorbed thiophene on sulfided Mo/Al_2O_3 catalysts (14 wt % MoO_3 before sulfidation). The catalysts were exposed to thiophene at room temperature prior to spectral acquisition at 20 K. On the basis of their interpretation of the INS spectra (400−2000 cm^{-1}), Mitchell et al.[3] concluded that thiophene is weakly chemisorbed to the catalyst surface, with 90−95% of the thiophene adsorbed in an η^5 geometry and the remaining 5−10% adsorbed in an η^1(S) geometry (see Figure 1). Bussell and co-workers[4] used infrared (IR) spectroscopy to examine the adsorption of thiophene on sulfided Mo/Al_2O_3 catalysts with a range of Mo loadings (14−39 wt % MoO_3). The catalysts were exposed to a saturation dose of thiophene at 190 K, followed by spectral acquisition at 140 K. In a second set of experiments, the catalysts were exposed to 5.0 Torr of thiophene at 298 K with subsequent spectral acquisition at this temperature. On the basis of the interpretation of the IR spectra

* To whom correspondence should be addressed. E-mail: Mark.Bussell@wwu.edu. Tel: 360-650-3145. Fax: 360-650-2826

10.1021/jp010258r CCC: $20.00
Published on Web 04/13/2001

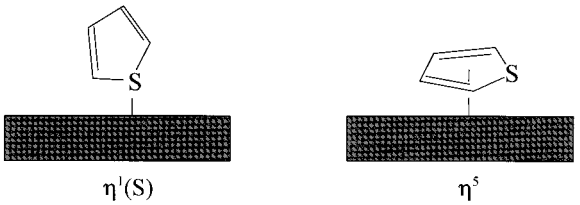

Figure 1. Proposed adsorption geometries for thiophene on sulfided Mo/Al_2O_3 catalysts.[3,4]

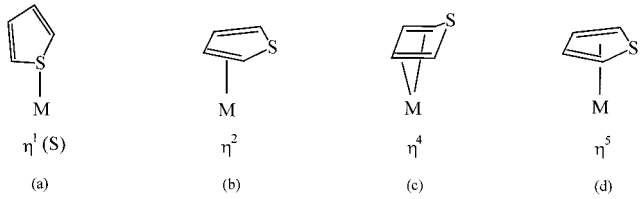

Figure 2. Modes of thiophene bonding in organometallic complexes.[7]

(1000−4000 cm^{-1}), thiophene was proposed to adsorb in an η^1(S) geometry to cus Mo sites located at the edges of MoS_2-like structures. Infrared spectra obtained in a subsequent study of thiophene adsorption on sulfided Rh/Al_2O_3 catalysts suggest that thiophene is also η^1(S)-bonded to cus Rh sites.[5]

In assigning IR spectral features to particular modes of thiophene adsorption, both Mitchell et al.[3] and Bussell and coworkers[4] used vibrational and/or structural data for organometallic complexes containing thiophene ligands. Organometallic chemistry has provided a wealth of information concerning the bonding of thiophene to metal centers.[6−8] Although metal centers in mononuclear organometallic complexes are not the same as sites in HDS catalysts, these complexes have the huge advantage that one knows from X-ray crystal structure data how the thiophene ligand is bonded to the metal atom. As shown in Figure 2, four different bonding modes have been observed for thiophene in organometallic complexes. In many cases, thiophene ligands in organometallic complexes have been observed to undergo reaction. Unfortunately, no conclusive evidence has yet been obtained indicating which coordinated thiophene species is a direct precursor to a C−S bond insertion or a desulfurization product. Experimental results point to η^1(S)-coordinated thiophene being the precursor to C−S bond cleavage,[9] although η^5-coordinated thiophene species also undergo C−S bond cleavage when attacked by a hydride ion,[10] a proton,[11] or a base.[12] In this paper, organometallic complexes serve as structural models of thiophene adsorbed at a metal site on an HDS catalyst but not as functional models because they do not catalyze HDS. The use of organometallic complexes as models for understanding molecular adsorption in a number of different systems has been reviewed elsewhere.[13]

A number of theoretical studies have been undertaken with regard to modeling the physical properties of gas phase, coordinated, and adsorbed thiophene. Scott[14] and Cyvin et al.[15] have performed complete normal coordinate analyses of free thiophene, whereas Orza et al.[16] have performed a similar analysis limited to the molecule's out-of-plane vibrational modes. More recently, electronic structure calculations of thiophene, as well as other five-membered heterocycles, have been performed by Simandiras et al.,[17] El-Azhary et al.,[18,19] and Kwiatkowski et al.,[20] whereas the electronic structure of thiophene ligands, coordinated in a variety of metal complexes, have been studied extensively by a number of researchers.[21−25] Modeling the properties of adsorbed thiophene has also received considerable attention. Most recently, Atter et al.[26] used a combined ab initio/normal coordinate approach to calculate the

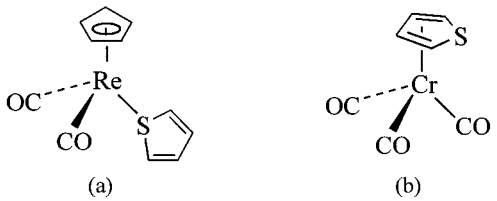

Figure 3. Chemical structures of (a) $(\eta^5\text{-}C_5D_5)Re(CO)_2(\eta^1\text{(S)-}C_4H_4S)$ and (b) $(\eta^5\text{-}C_4H_4S)Cr(CO)_3$.

INS spectrum of thiophene adsorbed on alumina and model HDS catalysts, whereas Rodriguez[27] and Toulhoat et al.[28] have used ab initio methods to investigate the bonding configuration of thiophene on MoS_2 surfaces.

Although the above studies offer some detailed insights into various properties of free, coordinated, and adsorbed thiophene, the relationship between the bond strengths (represented by a force field comprised of harmonic force constants) of adsorbed thiophene and the species' vibrational spectrum remains largely uninvestigated. Such work is of some interest, however, as the two likely η^1(S)- and η^5-bonding configurations thiophene may adopt, in either an organometallic complex or at a catalyst's surface, must necessarily possess dissimilar force fields, which in turn give rise to characteristic vibrational spectra. Thus, to gain a quantitative insight into which bonding mode thiophene adopts when adsorbed on cus Mo sites of sulfided Mo catalysts, a vibrational spectroscopic investigation of organometallic complexes possessing thiophene ligands, as well as a series of normal coordinate analyses of gas phase, η^1(S)- and η^5-coordinated thiophene, were undertaken. It is shown here that perturbations among the gas-phase species' force constants, necessary to model the corresponding observed infrared spectrum of the thiophene ligand in $(\eta^5\text{-}C_5D_5)Re(CO)_2(\eta^1\text{(S)-}C_4H_4S)$ (see Figure 3), confirms our previous interpretation that the adsorbed species is bound with an η^1(S)-coordination to cus Mo sites of sulfided Mo/Al_2O_3 catalysts.[4] A similar analysis of the infrared bands of the thiophene moiety in $(\eta^5\text{-}C_4H_4S)Cr(CO)_3$ (see Figure 3) shows that thiophene does not adsorb to cus Mo sites with an η^5 coordination under the conditions employed.

Experimental Section

General Procedures for the Syntheses of the η^1(S)- and η^5-C_4H_4S Complexes. All syntheses were performed under a nitrogen atmosphere using standard Schlenk techniques. Reagent grade solvents were used for all reactions. Hexanes and CH_2Cl_2 were dried over CaH_2 prior to use. Tetrahydrofuran (THF) and diethyl ether were dried and distilled over sodium benzophenone ketyl. Nitromethane was dried using $CaCl_2$, filtered and distilled prior to use. All deuterated solvents were stored over 3 Å molecular sieves. Neutral alumina (Brockmann, activity 1, 150 mesh), used for column chromatography, was degassed under vacuum ($P = 0.01$ Torr) for 12 h and then activated with 5 wt% N_2-saturated water with vigorous shaking. Thiophene (Aldrich Chemical Co.) was purified according to the procedure of Spies and Angelici.[29] Sodium sulfate and boron trifluoride etherate (Aldrich Chemical Co.) were used without further purification.

^{1}H NMR spectra were recorded on either a Varian VXR-300 or a Bruker DRX-400 MHz spectrometer using the appropriate deuterated solvent as internal lock, reference, and solvent. ^{2}D NMR spectra were recorded on a Bruker DRX-400 NMR spectrometer using CH_2Cl_2 as the solvent and C_6D_6 as the internal reference. The temperature of the photolysis reaction

was regulated using a Fischer Scientific ISOTEMP 1013P programmable circulating bath, with the circulation hoses connected to a 20 cm coldfinger which was immersed into the reaction solution.

C_5D_5Tl. The synthesis of C_5D_5Tl was adapted from that of Anderson et al.[30] A solution of sodium deuterioxide was prepared from freshly cut sodium (3.75 g, 0.16 mol) and D_2O (40 mL, 2.0 mol). Freshly distilled cyclopentadiene (0.65 mL, 7.89 mmol) was added to a solution of sodium deuterioxide (20 mL). The mixture was mechanically shaken (Fischer Vortex) for 4 h under argon atmosphere at room temperature. Cyclopentadiene was extracted with 1 mL of C_6D_6 and added to a second portion (20 mL) of the sodium deuterioxide solution. The mixture was shaken for another 4 h; then, thallium (I) sulfate (1.50 g, 2.97 mmol) was added, and the mixture was shaken overnight. The pale-brown solid product was filtered, dried under vacuum and sublimed at 383−393 K and 0.01 Torr to yield pure (99+% isotopic purity) C_5D_5Tl (0.97 g, 59%). MS (70 eV, EI): *m*/*z* 275 (M^+, ^{205}Tl), 273 (M^+, ^{203}Tl), 205 ($M^+ - C_5D_5$, ^{205}Tl), 203 ($M^+ - C_5D_5$, ^{203}Tl).

(η^5-C_5D_5)Re(CO)$_2$(η^1(S)-C_4H_4S) (1). This procedure is adapted from that previously reported for the preparation of (η^5-C_5H_5)Re(CO)$_2$(η^1(S)-C_4H_4S).[31] A THF (30 mL) solution of (η^5-C_5D_5)Re(CO)$_3$[32] (194 mg, 0.570 mmol) was prepared in a 60 mL capacity quartz photolysis tube, equipped with a stir bar. A coldfinger was immersed into the solution and the tube was irradiated (Hanovia 450 W Hg lamp) at 263 K for 3−4 h under a nitrogen atmosphere. The yellow−orange solution containing (η^5-C_5D_5)Re(CO)$_2$(THF) was then allowed to warm to room temperature, at which time thiophene (4.0 mL, 50 mmol) was added via a syringe. The solution was then stirred until the υ_{CO} bands corresponding to (η^5-C_5D_5)Re(CO)$_2$(η^1(S)-C_4H_4S) reached their maximum absorptions (10 h) as monitored by IR spectroscopy. After the solvent was removed in vacuo, the residue was extracted with CH_2Cl_2/hexanes (1:10) and separated via chromatography using an alumina column (1 cm × 12 cm) to remove unreacted starting materials. A yellow band corresponding to **1** was eluted and collected, and the solvent was reduced to 10 mL. Storage overnight at 253 K produced yellow crystals of **1** in 27% yield (60 mg). ^{1}H NMR ($CDCl_3$) 300 MHz: δ 7.28 (br, s, 2 H), 7.06 (br, s, 2 H). ^{2}H NMR (CH_2Cl_2) 61 MHz: δ 4.58 (s, 5 D, η^5-C_5D_5). IR (hexanes): υ_{CO}, cm^{-1} 1951 (s), 1889 (s).

(η^5-C_4H_4S)Cr(CO)$_3$ (2). The complex (η^5-C_4H_4S)Cr(CO)$_3$ was prepared using a modified version of a procedure described by Novi et al.[33] A diethyl ether (20 mL) slurry of tricarbonyltris-(pyridine)chromium[34] (276 mg, 0.740 mmol) was prepared in a 50 mL Schlenk flask equipped with a stir bar. Thiophene (2.0 mL, 25 mmol) and BF_3 etherate (0.30 mL) were then added successively to the slurry, via a syringe. After stirring for 20 min, diethyl ether (10 mL) was added, and the solution was cooled to 273 K followed by addition of deoxygenated water (4−5 mL) with stirring. The product was extracted with ether, washed with water and dried over Na_2SO_4. The solvent and unreacted thiophene were removed in vacuo, leaving an orange-red residue which was subsequently dissolved in hexanes−CH_2Cl_2 (5:1) and separated via column chromatography on alumina packed in hexanes (1 cm × 10 cm). An orange band was eluted and collected; the solvent was removed in vacuo to produce orange **2** which was recrystallized from CH_2Cl_2 and hexanes to afford orange crystals in 65% yield. ^{1}H NMR ($CDCl_3$) 300 MHz: δ 5.36 (m, 2 H), 5.58 (m, 2 H), IR (hexanes): υ_{CO}, cm^{-1} 1967 (s), 1884 (m) and 1869 (m).

[(η^5-C_4H_4S)Mn(CO)$_3$]BF_4. The procedure described by Chen and Angelici[35] was used without modification. ^{1}H NMR (d_6-acetone): δ 7.07 (m, 2 H), 7.25 (m, 2 H). IR (CH_3NO_2): υ_{CO}, cm^{-1} 2079 (s), 2017 (s, br).

Infrared and Raman Spectral Acquisition. Infrared and Raman spectra were acquired using a Bruker Equinox 55/FRA 106 FTIR/FT Raman system operated by Bruker OPUS 2.2 software. The infrared spectrometer is equipped with KBr and Mylar beam splitters for the near and far-infrared regions, respectively, and with a DTGS detector. The FT Raman module is equipped with a Nd:YAG laser (1064 nm) and a liquid nitrogen cooled Ge detector. For the infrared measurements (128 scans, 4 cm^{-1} resolution), the samples were diluted with CsI and pressed into pellets in a glovebox purged with dry nitrogen before being mounted in the spectrometer. For the Raman measurements, the pure samples were put into NMR tubes under an inert gas atmosphere and subsequently measured in the 180° scattering geometry (200 mW defocused beam, 4 cm^{-1} resolution).

Normal Mode Calculations. The normal mode calculations were performed using a program written by McIntosh and Peterson,[36] based on Wilson's FG matrix method.[37] Details pertaining to how such calculations are performed have been discussed elsewhere.[38] Briefly, the program utilizes a suite of three subprograms, UMAT, ATOM2, and FFIT. The first of these is used to generate the $\boldsymbol{F}^{sym}$ and $\boldsymbol{B}^{sym}$ matrices of the desired species' model. Such models are initially constructed from a description of the species' atomic coordinates, internal coordinates (including their respective initial force constants) and symmetry point group. The $\boldsymbol{F}^{sym}$ and $\boldsymbol{B}^{sym}$ matrices generated in this manner are subsequently employed by the ATOM2 program to derive descriptions of the species normal coordinates, in terms of the relative contributions from each member of the internal coordinate basis set and their respective calculated frequencies. This allows for the assignment of modes of known composition to their corresponding observed and calculated frequencies. The final program, FFIT, utilizes a simplex optimization algorithm to refine the components of the $\boldsymbol{F}^{sym}$ matrix via a nonlinear least-squares analysis between calculated and observed frequencies. Once a final solution is obtained in this manner, the optimized or "best fit" force constant parameters are re-run through both the UMAT and the ATOM2 programs in order to confirm the calculated frequency and composition of each of the model compound's normal modes.

Three normal coordinate analyses of the in-plane vibrations of thiophene were performed. Initially, an accurate model of the C_{2v} symmetry gas-phase species was constructed. The geometric parameters used for this thiophene model were taken from electron diffraction data,[39] whereas 20 initial force constants (10 diagonal and 10 off-diagonal), utilized in conjunction with 18 internal coordinates, were taken from a series of closely related compounds[14,40−43] or were approximated using an empirical approach based on Badger's rule.[44] The gas-phase species' force field was refined via the FFIT program, which was utilized to perform a nonlinear least-squares analysis between a total of 45 discrete experimental and calculated frequencies. The experimental frequencies were taken from the IR spectra of three C_{2v} symmetry C_4H_4S and $C_4H_2D_2S$ isotopomers.[18] As alluded to above, the composition of each normal mode and the values of their corresponding calculated frequencies were first checked by running this new set of optimized parameters through the UMAT and ATOM2 programs. As with

TABLE 1: Bond Lengths Å for Free and Coordinated Thiophene

compound	C(2) − S (Å)	C(5) − S (Å)	C(2) − C(3) (Å)	C(3) − C(4) (Å)	C(4)−C(5) (Å)	ref
free thiophene (T)	1.714 ± 0.001	1.714 ± 0.001	1.370 ± 0.002	1.424 ± 0.002	1.370 ± 0.002	39
			$\eta^1(S)$ - coordinated			
$(PPh_3)_2Ru(C_5H_4CH_2C_4H_3S)^+$	1.754 ± 0.006	1.734 ± 0.006	1.344 ± 0.008	1.409 ± 0.008	1.339 ± 0.008	45
$Cp(CO)(PPh_3)Ru(2\text{-}MeT)^+$	1.753 ± 0.005	1.756 ± 0.005	1.350 ± 0.007	1.417 ± 0.008	1.329 ± 0.008	46
			η^5 − coordinated			
$(CO_3)Cr(2,5\text{-}Me_2T)$	1.754 ± 0.002	1.758 ± 0.002	1.383 ± 0.003	1.422 ± 0.003	1.385 ± 0.003	47
$(C_8H_{12})Rh(2,5\text{-}Me_2T)$	1.764 ± 0.006	1.743 ± 0.006	1.409 ± 0.008	1.377 ± 0.008	1.390 ± 0.007	48
$(PPh_3)_2Rh(T)$	1.73 ± 0.01	1.73 ± 0.01	1.40 ± 0.02	1.38 ± 0.02	1.43 ± 0.02	49

each of the analyses discussed here, the validity of the optimized force field was further assessed using two additional criteria. First, the "best fit" solution was considered satisfactory when a root-mean-square (RMS) error of ≤ 30 cm^{-1} was achieved between the calculated and observed frequencies. Because the FG matrix method utilizes a harmonic description of the internal coordinates' potential energy, it is unrealistic to expect an accuracy of fit greater than the degree of error associated with the anharmonicity of the observed bands. Second, because the initial force constants were taken from compounds possessing analogous internal coordinates to those of the gas phase model of thiophene, the optimized force constants were considered physically reasonable if their values did not diverge significantly (10−20%) from these initial values upon optimization. Thus, the mathematical solution calculated was deemed representative of the physical system when each of these principle criteria was concurrently satisfied.

To model the infrared spectra of the thiophene moiety coordinated in either an η^1(S) or η^5 geometry, within $(\eta^5\text{-}C_5D_5)Re(CO)_2(\eta^1(S)\text{-}C_4H_4S)$ and $(\eta^5\text{-}C_4H_4S)Cr(CO)_3$, respectively, the force constants of the gas-phase thiophene model were perturbed in a manner consistent with each species' bonding mode. For the η^1(S)-thiophene species, the force constants for the model's C−S, C═C, and C−C internal coordinates were repeatedly adjusted in an incremental ratio of (−3%):(+1%):(+0.5%), respectively, until the calculated frequency shifts matched analogous divergences observed between the physical systems to within an RMS error of ≤ 50 cm^{-1}. The relative force constant step size increments were in turn chosen to reflect trends of bond length expansion and contraction observed for gas-phase thiophene, η^1(S)-coordinated thiophene in $(PPh_3)_2Ru(C_5H_4CH_2C_4H_3S)^+$,[45] and $Cp(CO)(PPh_3)Ru(2\text{-}MeC_4H_3S)^+$,[46] where Cp = η^5-cyclopentadienyl. Structural data for gas-phase thiophene as well as η^1(S)- and η^5-coordinated thiophene ligands are summarized in Table 1. For the η^1(S)-coordinated thiophene ligands, the C═C and C−C coordinates of these complexes are shown to shorten by averages of 0.0295 and 0.011 Å, respectively, whereas the C−S coordinates lengthen by an average of 0.0350 Å. In addition, perturbations among this model's force constants are also consistent with the electronic structure of thiophene η^1(S)-coordinated to metal centers as will be discussed later. Once in the vicinity of a solution, the η^1(S)-model's force field was further refined using the FFIT program.

A similar procedure was carried out for the η^5-thiophene species, with the force constants for the model's C−S, C═C and C−C internal coordinates each varied by (−1%):(−1%):(+0.5%) increments, respectively, before being further refined by the FFIT program. These stepwise force constant perturbations also reflect trends of bond length expansion and contraction, in this case observed between gas phase and η^5-coordinated thiophene in $(CO)_3Cr(2,5\text{-}Me_2C_4H_2S)$,[47] $(C_8H_{12})Rh(2,5\text{-}Me_2C_4H_2S)$[48] and $(PPh_3)_2Rh(C_4H_4S)$.[49] Structural data for the thiophene ligands in these complexes are listed in Table 1. The structural data represent a summary of the most accurate X-ray diffraction data published in the literature for organometallic complexes containing η^1(S)- and η^5-coordinated thiophene ligands. The C−S and C═C coordinates of thiophene in the η^5-coordinated complexes lengthen by averages of 0.033 and 0.030 Å, respectively, whereas the C−C coordinate shortens by an average of 0.031 Å. As with the η^1(S) thiophene complexes, the perturbations among the force constants for the η^5-coordinated thiophene ligand in the Cr complex are also consistent with the electronic structure of thiophene η^5-coordinated to metal centers as will be discussed later.

Results and Discussion

Spectral Analysis. Infrared and Raman spectra acquired for $(\eta^5\text{-}C_5D_5)Re(CO)_2(\eta^1(S)\text{-}C_4H_4S)$, $(\eta^5\text{-}C_4H_4S)Cr(CO)_3$, and $(\eta^5\text{-}C_4H_4S)Mn(CO)_3BF_4$ are shown in Figures 4 and 5, respectively, whereas the compounds' respective spectral assignments, as well as those of thiophene, are displayed in Table 2. Infrared bands of coordinated thiophene in each complex appearing below 600 cm^{-1} were assigned using complementary spectra acquired in the far-IR region which are not shown here. The assignments of nonthiophene bands appearing below 600 cm^{-1} are based on comparisons with the literature. Modes readily assigned to each complex's ν(CO) bands appear in the region 1836−2077 cm^{-1}, whereas the Mn complex displays bands attributed to $\nu(BF_4)$ modes in the range 1000−1200 cm^{-1}. The Re complex contains an η^5-coordinated Cp(d_5) ligand, which in turn gives rise to ν(CD) bands in the 2336−2448 cm^{-1} region. Deuteration of the Cp ligand allowed for differentiation between its own bands and those due to the thiophene moiety, which would have otherwise been obscured. This is particularly important, as many of the Cp ligand's ring modes give rise to bands at essentially identical frequencies to those of the analogous modes of thiophene. Deuteration of the Cp ligand not only shifts bands associated with C−H stretch modes to lower frequencies but also those associated with ring bend and stretch modes. In related studies reported by others, complete assignment of modes associated with thiophene ligands in the vibrational spectra of $[(\eta^5\text{-}C_5H_5)(CO)_2Fe(\eta^1(S)\text{-}3\text{-}MeC_4H_4S)]BF_4$[50] and $[(\eta^5\text{-}C_5H_5)(CO)_2Fe(\eta^1(S)\text{-}C_4H_4S)]BF_4$[3] was not possible due to the overlap of bands due to the thiophene and the nondeuterated Cp ligands. For $(\eta^5\text{-}C_5D_5)Re(CO)_2(\eta^1(S)\text{-}C_4H_4S)$, the origin of the weak bands observed at 2960 and ∼1305 cm^{-1} is unknown but may possibly be due to decomposition of a minor amount of the coordinated thiophene. With the exception of the bands discussed above, the remainder of the bands seen above ∼600 cm^{-1} (labeled 1−15 in Table 2) may be assigned to the in-plane vibrational modes of each compound's thiophene moiety. These assignments were further refined via a comparison with normal-mode analyses of η^1(S)- and η^5-coordinated thiophene, the results of which are discussed in the following section. Weak bands observed below ∼600 cm^{-1} were assigned to a variety of ring torsion and metal−ligand stretch or bend modes. For each complex, the initial band assignments were based on

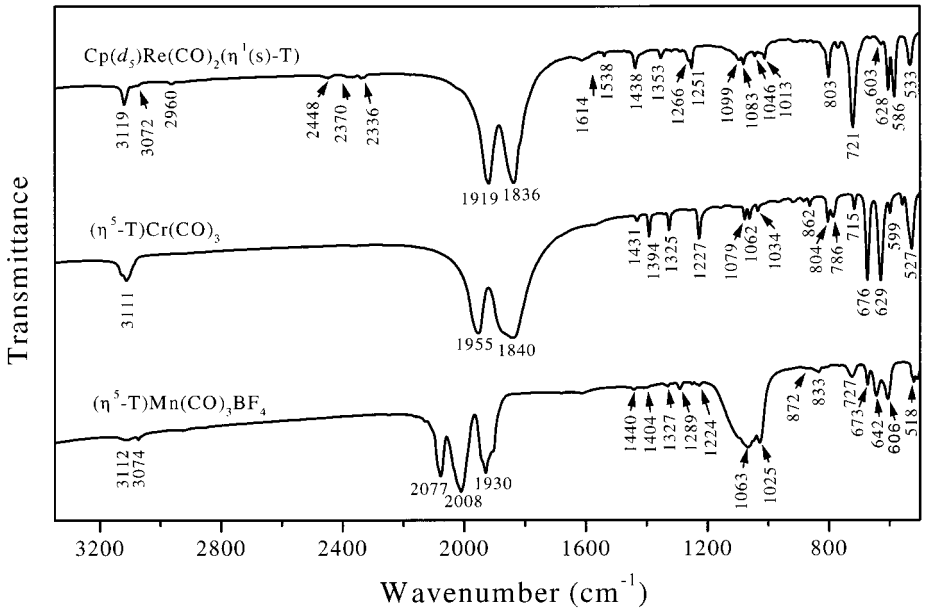

Figure 4. Infrared spectra of $(\eta^5\text{-}C_5D_5)Re(CO)_2(\eta^1(S)\text{-}C_4H_4S)$, $(\eta^5\text{-}C_4H_4S)Cr(CO)_3$, and $[(\eta^5\text{-}C_4H_4S)Mn(CO)_3]BF_4$.

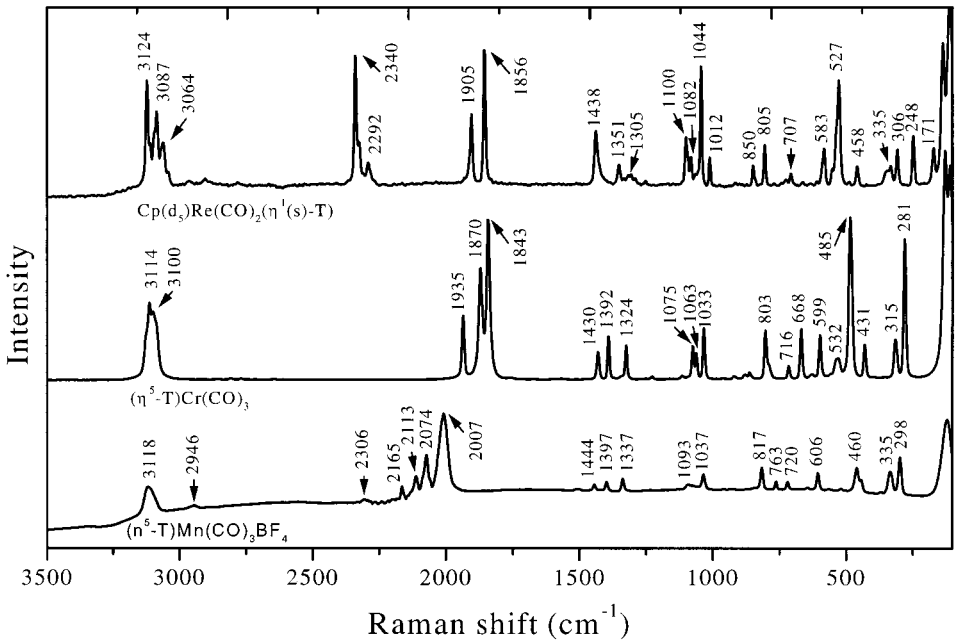

Figure 5. Raman spectra of $(\eta^5\text{-}C_5D_5)Re(CO)_2(\eta^1(S)\text{-}C_4H_4S)$, $(\eta^5\text{-}C_4H_4S)Cr(CO)_3$, and $[(\eta^5\text{-}C_4H_4S)Mn(CO)_3]BF_4$.

literature assignments of analogous compounds,[51−53] as well as through reference to the IR spectrum of free thiophene.[54]

Spectral shifts observed for a number of peaks in the vibrational spectra of the thiophene ligands in $(\eta^5\text{-}C_5D_5)Re(CO)_2(\eta^1(S)\text{-}C_4H_4S)$, $(\eta^5\text{-}C_4H_4S)Cr(CO)_3$, and $(\eta^5\text{-}C_4H_4S)Mn(CO)_3BF_4$, relative to gas-phase thiophene, are of significant interest. When compared to free thiophene, the $\nu(C{=}C)_{sym}$, $\nu(C{=}C)_{as}$, and "$\nu(C{-}C)$" bands of $\eta^1(S)$-coordinated thiophene in the Re complex are shifted by + 29, +31 and +10 cm^{-1} respectively, whereas the $\nu(C{-}S)$ band shifts by −123 cm^{-1} (i.e., in the opposite direction). The "$\nu(C{-}C)$" mode (mode #11), as is discussed in more detail below, is a nonlocalized ring stretching mode, but whose largest single contribution remains the stretching of the C−C internal coordinate. For this reason, we will refer to it as the "$\nu(C{-}C)$" mode. As discussed in more detail below, these observations are consistent with what is known of the electronic[21,22,25] and geometric structure of η^1-(S)-coordinated thiophene, where, with respect to the gas-phase species, electron density is increased within the C=C−C=C fragment while being significantly reduced in the C−S bonds. For η^5-coordinated thiophene in $(\eta^5\text{-}C_4H_4S)Cr(CO)_3$, all of the species' in-plane modes become shifted to lower frequencies with respect to gas-phase thiophene. For example, when compared to the gas phase, the thiophene ligand's $\nu(C{=}C)_{sym}$, $\nu(C{=}C)_{as}$, "$\nu(C{-}C)$", and $\nu(C{-}S)$ bands shift by −15, −76, −2, and −75 cm^{-1}, respectively. As discussed below, these observations are consistent with the proposed electronic[21,22] and geometric structure of η^5-coordinated thiophene, where, with respect to the gas-phase species, electron density is decreased over the entire thiophene ring. A similar trend is observed among the IR bands of η^5-coordinated thiophene in $[(\eta^5\text{-}C_4H_4S)Mn(CO)3]BF_4$, illustrating that the direction of the shifts, with

TABLE 2: Vibrational Mode Assignments for Gas Phase Thiophene and Re, Cr, and Mn Complexes

C_4H_4S mode	C_4H_4S(g) band freq (IR) (cm^{-1})	Re(η^1(S)-C_4H_4S) band freq (cm^{-1})	Cr(η^5-C_4H_4S) band freq (cm^{-1})	Mn(η^5-C_4H_4S) band freq (cm^{-1})	assignment
1	3126	3119 (IR)	3114 (R)	3112 (IR)	ν(CH)(α)
3	3098	3072 (IR)	3100 (R)	3074 (IR)	ν(CH)(β)
		2448 (IR)			ν(CD)(Cp)
		2370 (IR)			ν(CD)(Cp)
		2336 (IR)			ν(CD)(Cp)
		1919 (IR)	1935 (R)	2077 (IR)	ν(CO)
		1836 (IR)	1871 (R)	2008 (IR)	ν(CO)
			1843 (R)	1930 (IR)	ν(CO)
5	1507	1538 (IR)	1431 (IR)	1440 (IR)	ν(C═C)$_{asym}$
6	1409	1438 (IR)	1394 (IR)	1404 (IR)	ν(C═C)$_{sym}$
7	1360	1353 (IR)	1325 (IR)	1327 (IR)	ν(ring)
8	1256	1266 (IR)	1227 (IR)	1224 (IR)	ν(ring)
		1251 (IR)			ν(C═C)(Cp)
		1099 (IR)			ν(ring)(Cp)
9	1085	1083 (IR)	1079 (IR)	1093 (R)	δ(CH)$_{asym}$
10	1083		1062 (IR)		δ(CH)$_{sym}$
				1063 (IR)	ν(BF)
11	1036	1046 (IR)	1034 (IR)	1037 (R)	ν(ring)
				1025 (IR)	ν(BF)
		850 (R)			δ(CD)(Cp)
12	898				ρ_{wag} (CH)
13	872	803 (IR)	862 (IR)	872 (IR)	δ(ring)$_{defm}$
14	867				ρ_{wag} (CH)
15	839	707 (R)	804 (IR)	817 (R)	δ(ring)$_{defm}$
		772 (IR)			δ(CD)(Cp)
16	751	628 (IR)	676 (IR)	673 (IR)	ν(CS)$_{asym}$
				727 (IR)	δ(BF)
17	712	721 (IR)	786 (IR)		ρ_{wag} (CH)
18	683		715 (IR)	727 (IR)	ρ_{wag} (CH)(sh.)
			629 (IR)	642 (IR)	δ(M-CO)
19	608	545 (IR)	558 (IR)		δ(ring)$_{defm}$
			599 (IR)	606 (IR)	δ(M-CO)
		603 (IR)			δ(CD)(Cp)
20	565	586 (IR)	527 (IR)	518 (IR)	τ(ring)
21	452	488 (IR)	485 (IR)		τ(ring)
		459 (IR)			τ(ring)(Cp)
		410 (IR)	431 (IR)		ν(M-CO)
		351 (IR)			ν(Re−Cp)
			342 (IR)		ν(Cr-ring)
		307 (IR)			ν(Re−Cp)
			283 (IR)		ν(Cr-ring)
		246 (IR)			ν(Re−S)
		137 (IR)			δ(Re−Cp)
			132 (IR)		δ(Cr-ring)
		119 (IR)			δ(Re−Cp)
			113 (IR)		δ(Cr-ring)
		111 (IR)			δ(Re−S)

respect to gas-phase thiophene, depends on the bonding geometry of the thiophene ligand, rather than the chemical identity of the coordinated metal species. However, the magnitude of the shifts seen for η^5-coordinated thiophene in the Mn complex differs slightly from those of the analogous Cr coordinated thiophene ligand. For example, the ν(C═C)$_{sym}$, ν(C═C)$_{as}$, "ν(C−C)", and ν(C−S) IR bands shift by −5, −67, −11, and −78 cm^{-1}, respectively, compared to free thiophene, whereas their absolute values differ by +10, +9, −9, and −3 cm^{-1} with respect to the analogous bands of the Cr coordinated ligand. These disparities are assumed to be due to the different oxidation states of the Mn(I) and Cr(0) centers.

The IR spectra of η^1(S)- and η^5-coordinated thiophene, found in (η^5-C_5D_5)Re(CO)$_2$(η^1(S)-C_4H_4S) and (η^5-C_4H_4S)Cr(CO)$_3$ respectively, were subjected to the normal-mode analyses discussed below. Because these theoretical results were subsequently used to determine the bonding configuration adsorbed thiophene adopts at the surface of a sulfided Mo/Al_2O_3 catalyst, the complementary Raman spectra of these complexes, shown in Figure 3, were not analyzed in similar detail. However, the Raman spectra of each complex proved essential in determining initial spectral assignments for the complexes. Specifically, because asymmetric Raman bands are generally attenuated with respect to their symmetric counterparts, several bands were initially assigned on the basis of symmetry and/or intensity considerations. Also, the inherently narrow line width of the Raman bands allowed for the unambiguous assignment of poorly resolved analogous spectral features in the corresponding IR spectra.

Normal Mode Calculations. Listed in Table 3 are the experimental and calculated vibrational frequencies derived for gas-phase thiophene (C_4H_4S), as well as for two partially deuterated $C_4H_2D_2S$ analogues. Deuteration at the α (C1, C4) and β (C2, C3) positions of C_4H_4S results in the formation of two distinct isotopomers, which retain the original species' molecular symmetry. This allowed for a normal coordinate analysis of these isotopomers to be conducted under a common C_{2v} symmetry, the results of which are presented here. As illustrated in Table 3, the observed and calculated frequencies of these d_0-, d_2(α)-, and d_2(β)-substituted thiophene isotopomers are in good agreement, with RMS error values of 7, 21, and 29 cm^{-1}, respectively. Because a vibrational mode's degree of

TABLE 3: Calculated and Experimental In−Plane Vibrational Frequencies (in cm^{-1}) for Thiophene Isotopomers[a]

mode	symmetry		C_4H_4S	$C_4H_2(D_{2\alpha})S$	$C_4H_2(D_{2\beta})S$
1	A_1	calcd	3129	2325	3129
		exp	3126	2336	3123
2	B_1	calcd	3126	2319	3127
		exp	3125	2326	3120
3	B_1	calcd	3098	3097	2318
		exp	3098	3088	2317
4	A_1	calcd	3093	3093	2302
		exp	3098	3101	2314
5	B_1	calcd	1512	1499	1438
		exp	1507	1490	1480
6	A_1	calcd	1417	1402	1374
		exp	1409	1398	1389
7	A_1	calcd	1351	1314	1332
		exp	1360	1310	1322
8	B_1	calcd	1259	1208	953
		exp	1256	1218	918
9	B_1	calcd	1086	746	1238
		exp	1085	770	1178
10	A_1	calcd	1071	716	725
		exp	1083	754	750
11	A_1	calcd	1028	1022	1043
		exp	1036	1046	1034
13	B_1	calcd	882	969	779
		exp	872	918	849
15	A_1	calcd	835	919	880
		exp	839	884	876
16	B_1	calcd	742	728	720
		exp	751	740	713
19	A_1	calcd	597	576	586
		exp	608	590	593

[a] Note that modes 12, 14, 17, and 18 are composed of out-of-plane ρ_w(CH) wag motions. Modes 20 and 21 are composed of out-of-plane τ(ring) torsion motions

anharmonicity increases with the level of molecular deuteration, one would expect a similar trend in RMS error with respect to d_0-d_2 substitution, as is seen here. Due to the relatively large degree of anharmonic error associated with complete deuteration, and in the interest of retaining a common, self-consistent force field for the three isotopomers investigated, the d_4-substituted thiophene species was not modeled. However, omission of this species from the calculation did not significantly degrade the quality of the fitting procedure. Because 45 calculated frequencies were fitted to their respective experimental values by varying only 20 force constant parameters, the force constant values returned by the optimization were deemed to be reliable.

The internal coordinate components utilized in modeling the force field of gas phase thiophene, as well as their respective force constant values, are displayed in Table 4. The choice of internal coordinates utilized in the basis set was determined by several criteria. Because thiophene is a ring system, its respective model contains a relatively large number of redundant coordinates. For example, the C−H (α position) bends may be described through displacement of either the C═C−H or S−C−H internal coordinates. Therefore, the calculation was simplified by selecting a reduced number of basis set components that avoid such redundancies, whereas also adequately describing all the possible vibrational displacements of the model. As is also shown in Table 4, the elimination of such redundant internal coordinates, as well as their respective force constants, allowed for the inclusion of 10 additional coupling constants. It was necessary to include as many significant off-diagonal elements (or coupling constants) as the program allows because, as is discussed further below, the stretch and/or bend components constituting each normal mode can become highly coupled due to the delocalized nature of the thiophene ring. As is evident from an inspection of the percent difference values (contained within parentheses) in Table 4, the respective initial and final (optimized) force constants of the gas-phase model diverge by an average of 22.5% from their initial values. It should be noted that, due to the lack of available initial force constant data in the literature for "ring" internal coordinates, this average error is somewhat inflated when compared with similar studies.[38,55] However, when viewed in the context of a concomitant 19 cm^{-1} average RMS error frequency fit, this deviation among the initial and optimized force constants supports the conclusion that the force field is physically reasonable, and therefore, that the normal coordinate analysis of thiophene is valid. Interestingly, differences between the initial and optimized force constants of the gas-phase model are consistent with the delocalized nature of the thiophene ring. Specifically, the force constants for the C−C and C−S "single" bonds increase by 4.5% and 16%, respectively, thereby gaining more "double" bond character, whereas, in contrast, the C═C "double" bond force constants weaken by 15%. These trends in turn underscore the importance of including the maximum number of allowed off-diagonal elements in the $\boldsymbol{F}^{sym}$ matrix because a convergence of the C−C, C−S, and C═C internal coordinates' force constant values indicates, in turn, that they are more likely to undergo significant coupling.

Although the thiophene mode assignments determined in this study, shown in Table 2, are consistent with reports in the literature,[18,54] the FG matrix methodology also allows for a further, more detailed, analysis of the composition of each normal mode in terms of relative contributions from each of its internal coordinate components. The composition of each normal mode, as defined by the potential energy distribution (PED) matrix, supports a delocalized picture of the thiophene ring. For example, mode 5 (which gives rise to the ν(C═C)$_{as}$ band), although principally composed of C═C stretch internal coordinates (51%), also contains significant contributions from C═C−C (21%) and C═C−H (17%) bend coordinates. The degree of ring delocalization, as represented by an increased mixed composition of each normal mode in terms of its component internal coordinates, is more pronounced for modes 7−11, which in turn give rise to bands in the mid-IR region. With the exception of modes 9 and 10 (which are only composed of C═C−H bend coordinates), each of these modes contains between 45% and 13% contributions from C═C and C−C stretch, as well as C═C−H bend, internal coordinates. Thus, modes 7, 8, and 11 may best be described as "ring stretch" modes.

The extent to which the force constants of the gas phase species model were perturbed in order to effectively calculate bands due to the thiophene coordinated in (η^5-C_5D_5)Re(CO)$_2$-(η^1(S)-C_4H_4S) and (η^5-C_4H_4S)Cr(CO)$_3$ are also illustrated in Table 4. Although the optimized force constants determined for the thiophene ligands are not necessarily unique, they are consistent with experimentally observed changes in the bond lengths as well as the results of electronic structure calculations as described below. For the η^1(S)-coordinated species, the C−S coordinate weakens by 37% with respect to the gas phase, whereas the C═C and C−C coordinates strengthen by 11% and 5.0%, respectively. Similarly, the C═C−S and C−S−C bend coordinates' force constants reduce by 44 and 15% respectively, whereas the C═C−C coordinate increases slightly by 4.5%. Reference to the structural data in Table 1 shows that the C═C and C−C coordinates of η^1(S)-coordinated thiophene ligands shorten by averages of 0.0295 and 0.011 Å, respectively,

TABLE 4: Force Constants for Gas Phase and Coordinated Thiophene Models[h]

internal coordinate	initial force constant[g]	C_4H_4S (g)[g]	η^1(S)-C_4H_4S[g]	η^5-C_4H_4S[g]
		stretches		
ν(C−S)	3.689[a]	4.262 00 (16)	2.685 06 (−37)	4.026 31 (−5.5)
ν(C═C)	7.506[a]	6.413 22 (−15)	7.118 67 (11)	6.066 30 (−5.4)
ν(C−C)	5.385[a]	5.626 40 (435)	5.907 72 (5.0)	5.721 69 (1.7)
ν(C−H)α	5.314[b]	5.277 27 (−0.7)	5.277 27 (0.0)	5.229 27 (−0.9)
ν(C−H)β	5.193[b]	5.153 42 (−0.8)	5.082 86 (−1.4)	5.169 94 (0.3)
		bends		
δ(C═C−H)α	0.513[c]	0.779 841 (52)	0.779 841 (0.0)	0.731 092 (−6.3)
δ(C═C−H)β	0.525[d]	0.815 699 (55)	0.815 690 (0.0)	0.840 590 (3.1)
δ(C═C−C)	1.250[d]	1.759 240 (41)	1.838 410 (4.5)	1.255 470 (−29)
δ(C═C−S)	1.173[b]	1.207 300 (2.9)	0.676 088 (−44)	1.207 300 (0.0)
δ(C−S−C)	1.596[b]	2.180 090 (36)	1.853 080 (−15)	1.752 570 (−20)
		stretch−stretch		
ν(C−S)/ν(C−S)	0.215[b]	0.122 360 (−43)	0.122 360 (0.0)	0.060 955 (−50)
ν(C═C)/ν(C═C)	−0.100[d]	−0.016 790 (−83)	−0.016 790 (0.0)	0.105 210 (−727)
ν(C═C)/ν(C−S)	0.450[e]	0.248 663 (−45)	0.248 663 (0.0)	0.248 663 (0.0)
ν(C═C)/ν(C−C)	0.397[e]	0.416 026 (4.8)	0.415 026 (−0.2)	0.415 026 (−0.2)
		bend−stretch		
ν(C═C)/δ(C═C−H)α	0.197[c]	0.200 979 (2.0)	0.200 979 (0.0)	0.200 979 (0.0)
ν(C═C)/δ(C═C−H)β	0.232[f]	0.572 827 (147)	0.572 827 (0.0)	0.572 827 (0.0)
ν(C−S)/δ(C═C−H)β	−0.115[b]	−0.212 357 (42)	−0.212 357 (0.0)	−0.212 357 (0.0)
ν(C−C)/δ(C═C−H)α	0.115[b]	0.135 295 (−10)	0.135 297 (0.0)	0.135 295 (0.0)
ν(C−C)/δ(C═C−H)β	−0.115[b]	−0.439 505 (193)	−0.433 141 (−1.4)	−0.439 505 (0.0)
		bend−bend		
δ(C═C−H)/δ(C═C−H)	0.008[f]	−0.003 761 (−147)	−0.003 761 (0.0)	0.001 699 (−145)

[a] Initial force constants derived using a fitting procedure based on Badger's rule.[44] [b] Ref 14. [c] Ref 40. [d] Ref 41. [e] Ref 42. [f] Ref 58. [g] Stretch and bend force constants have units of mdyneÅ^{-1} and mdyneÅ^{-1}rad^{-2}, respectively. [h] Values in parentheses are the percent differences between the initial and the final (optimized) force constants.

whereas the C−S coordinates lengthen by an average of 0.0350 Å. In contrast, the normal coordinate analyses for the η^5-coordinated species reveal that the force constants of this model undergo a significantly different mode of perturbation to that of η^1(S)-coordinated thiophene. Specifically, the C−S and C═C coordinates' force constants decrease in magnitude by 5.5 and 5.4% respectively, whereas the C−C coordinate's force constant increases by 1.7%. These results are consistent with the structural data in Table 1, where the C−S and C═C coordinates of η^5-coordinated thiophene ligands are shown to lengthen by averages of 0.033 and 0.030 Å, respectively, whereas the C−C coordinate shortens by an average of 0.031 Å with respect to gas-phase thiophene. For each of the gas phase, η^1(S)- and η^5-coordinated thiophene species, the final optimized C−H coordinates' force constants vary little with respect to their initial values. This illustrates the fact that the established initial literature values are accurate and that the C−H stretch coordinates are essentially decoupled from the remainder of the molecule. An examination of each model's PED matrix confirms the later point, as each ν(CH) normal mode is comprised of ∼99% contributions from respective C−H internal coordinates.

As Table 5 illustrates, the calculated and observed frequencies for both the η^1(S)- and η^5-coordinated thiophene species are in close agreement. For the η^1(S)-coordinated species, a RMS error of 5 cm^{-1} is recorded, whereas for the η^5-coordinated fragment a RMS error of 6 cm^{-1} is returned. These results clearly illustrate that the IR spectra of each ligand may be accurately modeled by perturbing the gas-phase model's ***F*** matrix in a manner consistent with the proposed electronic structure of η^1(S)- and η^5-coordinated thiophene.

Comparison with Electronic Structure Calculations for η^1(S)- and η^5-Coordinated Thiophene Ligands. The analysis of the vibrational spectra for (η^5-C_5D_5)Re(CO)$_2$(η^1(S)-C_4H_4S), (η^5-C_4H_4S)Cr(CO)$_3$, and (η^5-C_4H_4S)Mn(CO)$_3$BF$_4$ as well as the perturbations among thiophene's force constants necessary to model the IR spectra of the thiophene ligands are consistent with electronic structure calculations carried out by others. Harris used Fenske−Hall type calculations to investigate the electronic structure of thiophene ligands in three complexes of interest: Cp*Re(CO)$_2$(η^1(S)-C_4H_4S)] where Cp* = η^5-pentamethylcyclopentadienyl,[22] (η^5-C_4H_4S)Cr(CO)$_3$,[21] and (η^5-C_4H_4S)Mn(CO)$_3^+$.[21] Density functional theory (DFT) was used by Sargent et al.[25] to examine thiophene η^1(S)-coordinated to Cp*Rh(P(CH$_3$)$_3$) and Cp*Re(CO)$_2$. The calculations by Harris indicate that η^5-coordination of thiophene in (η^5-C_4H_4S)Cr(CO)$_3$ and (η^5-C_4H_4S)Mn(CO)$_3^+$ causes only slight electron density perturbation, spread over the whole ring. Harris' calculations indicate that the 1a$_2$ and 2b$_1$ orbitals of thiophene can donate electron density to the metal whereas the empty 3b$_1$ and 2a$_2$ orbitals on thiophene can accept electron density from the metal. Donation of electron density from the 1a$_2$ orbital on thiophene to Cr would lead to weakening of the C═C bonds as would back-donation of electron density from Cr into the empty 3b$_1$ orbital of thiophene. This finding is consistent with the perturbations among thiophene's force constants necessary to model the IR spectrum of the η^5-coordinated thiophene ligand in (η^5-C_4H_4S)Cr(CO)$_3$. In particular, the normal coordinate analysis revealed that the force constant for the C═C coordinate decreased by 5.4% (relative to gas-phase thiophene) for the η^5-coordinated thiophene ligand in the Cr complex.

Electronic structure calculations for η^1(S) thiophene complexes are consistent with the results of the normal coordinate analyses of the thiophene ligand in (η^5-C_5D_5)Re(CO)$_2$(η^1(S)-C_4H_4S) as well. Harris used Fenske−Hall calculations to investigate the thiophene ligand in Cp*Re(CO)$_2$(η^1(S)-C_4H_4S) and several other η^1(S) complexes of thiophene.[21,22] Bonding through the sulfur atom was observed to be pyramidal, resulting in a nonplanar structure for the η^1(S)-coordinated thiophene, as observed experimentally for η^1(S) complexes and shown schematically in Figure 2. Harris' calculations revealed that thiophene, when η^1(S)-coordinated to a metal, can donate electron density to the metal via σ or π donation from the 2b$_1$

TABLE 5: Vibrational Mode Assignments for Gas Phase and Coordinated Thiophene

C_4H_4S mode		C_4H_4S(g) band freq (IR)[a] (cm^{-1})	Re(η^1(S)-C_4H_4S) band freq[b] (cm^{-1})	Cr(η^5-C_4H_4S) band freq[c] (cm^{-1})	Mn(η^5-C_4H_4S) band freq[d] (cm^{-1})	assignment
1	calcd	3129	3128	3114		ν(CH)(α)
	exp	3126	3119 (m)	3111 (m)	3112 (w)	
3	calcd	3098	3078	3098		ν(CH)(β)
	exp	3098	3072 (vw)		3074 (w)	
5	calcd	1512	1530	1441		$\nu(C{=}C)_{asym}$
	exp	1507	1538 (w)	1431 (w)	1440 (w)	
6	calcd	1417	1441	1387		$\nu(C{=}C)_{sym}$
	exp	1409	1438 (m)	1394 (m)	1404 (vw)	
7	calcd	1351	1349	1332		ν(ring)
	exp	1360	1353 (w)	1325 (m)	1327 (vw)	
8	calcd	1259	1267	1228		ν(ring)
	exp	1256	1266 (w)	1227 (m)	1224 (vw)	
9	calcd	1086	1085	1072		$\delta(CH)_{asym}$
	exp	1085	1083 (m)	1079 (w)		
10	calcd	1071	1074	1060		$\delta(CH)_{sym}$
	exp	1083		1062 (w)		
11	calcd	1028	1039	1025		ν(ring)
	exp	1036	1046 (w)	1034 (w)		
12	exp	898				ρ_{wag}(CH)
13	calcd	882	812	852		$\delta(ring)_{defm}$
	exp	872	803 (m)	862 (w)	872 (vw)	
14	exp	867				ρ_{wag}(CH)
15	exp	839	707[e]	804 (w)		$\delta(ring)_{defm}$
16	calcd	742	630	675		$\nu(CS)_{asym}$
	exp	751	628 (vw)	676 (s)	673 (w)	
17	exp	712	721 (s)	786 (m)		ρ_{wag}(CH)
18	exp	683		715 (w)	727 (w)	ρ_{wag}(CH)
19	calcd	597	526	563		$\delta(ring)_{defm}$
	exp	608	545 (m)	558 (w)		
20	exp	565	586 (s)	527 (m)	518 (w)	τ(ring)
21	exp	452	488 (m)	485 (s)		τ(ring)

[a] Ref 54. [b] This work. [c] Ref 51. [d] This work. [e] On the basis of the corresponding Raman band.

and $1a_1$ orbitals, respectively, and act as a π acceptor of electron density from the metal via the $3b_1$ orbital. Bonding of thiophene with the metal was observed to be dominated by donation of electron density from the $1a_1$ orbital of thiophene to the metal, with back-donation of electron density from the metal to the $3b_1$ orbital also contributing to the metal-sulfur bond for the Re complex. Back-donation of electron density into the $3b_1$ orbital on thiophene would result in weakening of both the C−S and C═C bonds.

Sargent et al.[25] used density functional theory to examine the electronic structure of thiophene η^1(S)-coordinated to CpRh(PMe$_3$) as well as to Cp*Re(CO)$_2$. The DFT results are generally consistent with those of Harris, but show some subtle differences. For thiophene η^1(S)-coordinated to CpRh(PMe$_3$), 0.26 e^- is donated from a sulfur lone pair fragment molecular orbital (FMO) on thiophene formed from a linear combination of the $2a_1$ ($1a_1$ in Harris' work) and $2b_1$ orbitals. This FMO has slight antibonding character for the C═C coordinates and donation of electron density to the metal from this orbital would be expected to strengthen the C═C bonds of thiophene. Back-donation of 0.15 e^- from the metal to the empty $2b_2$ orbital of thiophene is also observed for thiophene η^1(S)-coordinated to CpRh(PMe$_3$). The $2b_2$ orbital, not included in Harris' molecular orbital diagram, is also slightly antibonding for the C═C coordinates and back-donation of electron density into it would weaken the C═C bonds. For thiophene η^1(S)-coordinated to Cp*Re(CO)$_2$, the DFT calculations of Sargent et al.[25] show ligand to metal donation dominates the bonding, with 0.37 e^- donated from the sulfur lone pair FMO to the metal, and only 0.1 e^- back-donated from the metal to the $2b_2$ orbital of thiophene. One would expect, therefore, a slight strengthening of the C═C bonds due to the transfer of electron density from a filled thiophene FMO having C═C antibonding character and little back-donation into an empty FMO having C═C antibonding character. This observation is consistent with the normal-mode analyses in this work which show the force constants for the C═C bonds of the η^1(S)-coordinated thiophene ligand in (η^5-C_5D_5)Re(CO)$_2$(η^1(S)-C_4H_4S) increase 11% relative to gas-phase thiophene.

Comparison with Thiophene Adsorbed on Sulfided Mo/Al_2O_3 Catalysts. As described briefly in the Introduction, two vibrational spectroscopic studies of adsorbed thiophene on sulfided Mo/Al_2O_3 catalysts have recently been published.[3,4] In their study, Mitchell and co-workers[3] used INS spectroscopy which is highly sensitive to vibrational modes involving hydrogen and much less sensitive to modes involving other atoms. As a result, the INS spectra (400−2000 cm^{-1}) presented of thiophene adsorbed on a sulfided Mo/Al_2O_3 catalyst, as well as in (η^5-C_4H_4S)Cr(CO)$_3$, [(η^5-C_4H_4S)Mn(CO)$_3$]CF_3SO_3, and [(η^5-C_5H_5)(CO)$_2$Fe(η^1(S)-C_4H_4S)]BF_4 complexes,[3] show significant band intensity for only a limited number of vibrational modes. For example, the $\nu(C{=}C)_{sym}$ mode, which we show in this study to be sensitive to the mode of thiophene bonding, is not discernible in the INS spectra. Mitchell and co-workers[3] conclude that 90−95% of thiophene adsorbed on a sulfided Mo/Al_2O_3 catalyst under the conditions of their experiment (see Introduction) adopts an η^5 geometry based principally upon shifts of thiophene's out-of-plane C−H modes. These authors conclude that out-of-plane C−H wag modes, located at 702 and 740 cm^{-1} in their INS spectrum of pure thiophene solid, shift to higher wavenumbers for the Cr and Mn complexes which contain η^5-coordinated thiophene, and to lower wavenumbers in the Fe complex which contains η^1(S)-coordinated thiophene. In our judgment, however, a conclusive assignment of the out-of-plane C−H wag modes of the Fe complex cannot be made due to overlap with these same modes of the Cp ligand. In fact,

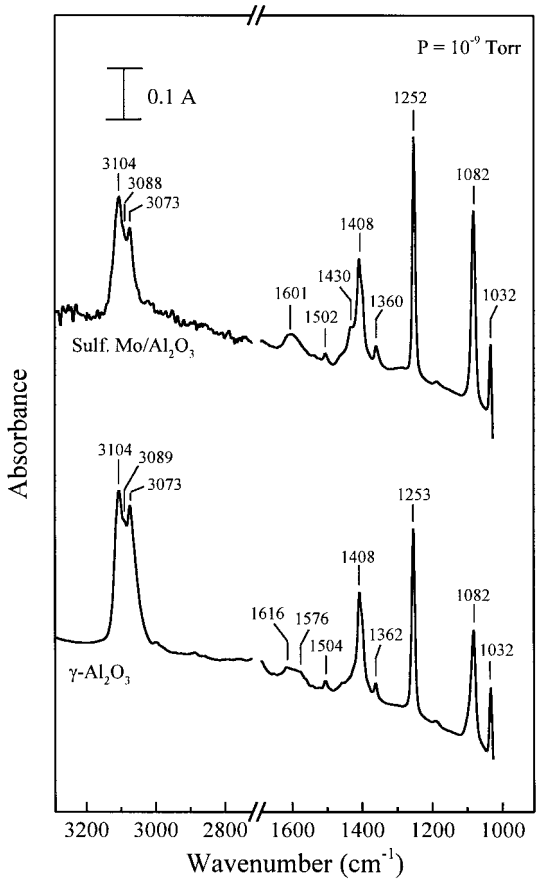

Figure 6. Infrared spectra of thiophene on ($-Al_2O_3$ and a sulfided Mo/Al_2O_3 catalyst (27.3 wt % MoO_3 in precursor).[4] The IR spectra were acquired in UHV at a sample temperature of 140 K.

our interpretation of the IR spectrum of $(\eta^5\text{-}C_5D_5)Re(CO)_2(\eta^1\text{-}(S)\text{-}C_4H_4S)$ indicates that the out-of-plane C−H wag mode observed for the η^1(S)-coordinated thiophene ligand is shifted to a higher wavenumber (721 cm^{-1}) from where it is located for pure thiophene gas, 712 cm^{-1}.[54] We conclude, therefore, that the position of the out-of-plane C−H wag modes cannot be used to conclusively distinguish between η^1(S)- and η^5-bonding geometries of thiophene adsorbed on sulfided Mo/Al_2O_3 catalysts.

Shown in Figure 6 are IR spectra acquired by Bussell and co-workers[4] for thiophene adsorbed on γ-Al_2O_3 and on a sulfided Mo/Al_2O_3 catalyst (27.3 wt % MoO_3). As described in detail elsewhere,[4] the IR spectra were acquired at a catalyst temperature of 140 K following a saturation dose of thiophene at 190 K. The IR spectrum of thiophene on the sulfided Mo/Al_2O_3 catalyst is a composite spectrum of thiophene adsorbed on cus Mo sites as well as on sites of the alumina support. Because the alumina sites are much greater in number than the cus Mo sites which are located along the edge planes of the supported MoS_2-like structures, the peaks associated with thiophene adsorbed on the uncovered alumina portion of the catalyst are much greater in intensity. Focusing initially on the IR spectrum of thiophene adsorbed on the pure γ-Al_2O_3 support, the peaks are essentially unshifted from their values for gas and liquid-phase thiophene.[4,54] Of particular importance, the $\nu(C{=}C)_{sym}$ mode is located at 1408 cm^{-1}, effectively unchanged from the gas-phase value of 1409 cm^{-1}. Examination of the IR spectrum for thiophene adsorbed on the sulfided Mo/Al_2O_3 catalyst reveals a new peak located at 1430 cm^{-1}. The absorbance feature at 1430 cm^{-1} was observed to grow in intensity with increasing Mo loading (14−39 wt % MoO_3) and to diminish when CO was dosed onto the catalyst prior to exposure to thiophene.[4] There is agreement in the literature that CO adsorbs to cus Mo sites located at the edges of MoS_2-like structures of sulfided Mo/Al_2O_3 catalysts.[2,56] Preadsorption of CO onto these sites blocks thiophene adsorption, which is reflected in a loss of spectral intensity of the 1430 cm^{-1} absorbance in the IR spectrum of sulfided Mo/Al_2O_3 catalysts exposed to thiophene. On the basis of the shift of the $\nu(C{=}C)_{sym}$ mode, Tarbuck et al.[4] concluded that thiophene adsorbs in an η^1(S) geometry at cus Mo sites located at the edges of MoS_2-like structures. Qualitative confirmation of the assignment of the adsorption mode to be η^1(S) was possible on the basis of molecular orbital and X-ray diffraction results reviewed in previous sections.

The results presented here support the above conclusions of Bussell and co-workers,[4] and make possible a more definitive assignment of the bonding geometry of thiophene adsorbed on sulfided Mo/Al_2O_3 catalysts. Our assignments of the vibrational bands in the IR spectra of $(\eta^5\text{-}C_4H_4S)Cr(CO)_3$, $(\eta^5\text{-}C_5D_5)Re(CO)_2(\eta^1(S)\text{-}C_4H_4S)$ and $[(\eta^5\text{-}C_4H_4S)Mn(CO)_3]BF_4$ indicate that the frequency of the $\nu(C{=}C)_{sym}$ mode of the thiophene ligand is indeed sensitive to the bonding mode, as observed here for thiophene coordinated to a metal center. As shown in the IR spectra (Figure 2), the $\nu(C{=}C)_{sym}$ mode shifts from its value for gas-phase thiophene (1409 cm^{-1}) to a higher frequency in the Re complex (1438 cm^{-1}) in which thiophene is η^1(S)-coordinated, and to lower frequencies in the Cr and Mn complexes (1394 and 1400 cm^{-1}, respectively) in which thiophene is η^5-coordinated. These observations provide additional, strong evidence for our previous assignment of the adsorption mode of thiophene on sulfided Mo/Al_2O_3 catalysts (in which case the $\nu(C{=}C)_{sym}$ mode of thiophene is observed at 1430 cm^{-1}) to be η^1(S).[4] As reviewed previously,[4,57] it is well-known that the frequencies of ring stretching modes of heterocyclic aromatic molecules are sensitive to their bonding environment on a catalyst surface. For example, the band position of the 8a mode of pyridine, which involves the symmetric stretching of the α-CC bonds[58] and is similar to the $\nu(C{=}C)_{sym}$ mode of thiophene, shifts 43 cm^{-1} higher than its value in pure liquid pyridine when pyridine is adsorbed via its N atom (η^1(N) geometry) to cus Al^{3+} sites of γ-Al_2O_3.[59]

Our assignment of the adsorption mode of thiophene on sulfided Mo/Al_2O_3 catalysts is also supported by the normal mode calculations reported here. As illustrated earlier, the IR spectrum of η^1(S)-coordinated thiophene, as observed for the ligand in $(\eta^5\text{-}C_5D_5)Re(CO)_2(\eta^1(S)\text{-}C_4H_4S)$, can only be modeled through a perturbation of the respective model's force constants consistent with a slight increase of electron density within the thiophene ligand's C=C−C=C fragment (11% and 5% for C=C and C−C bonds, respectively) and a concomitant depletion of electron density within the species' C−S coordinates (37%). Thus, the shift to higher frequency (with respect to the gas phase), observed for the $\nu(C{=}C)_{sym}$ mode of thiophene adsorbed at the cus Mo sites of sulfided Mo/Al_2O_3 catalysts, is attributed to η^1(S)-coordinated thiophene. The IR spectra of thiophene adsorbed at the sulfided Mo/Al_2O_3 catalyst's surface cannot be emulated using an η^5-coordinated thiophene model. As shown above, force constant perturbations necessary to model the IR spectra of η^5-coordinated thiophene in $(\eta^5\text{-}C_4H_4S)Cr(CO)_3$ are consistent with a reduction in electron density over the entire thiophene ring, as one may expect for an η^5-coordinated ligand. This general reduction in electron density over the thiophene ligand's ring manifests itself in a systematic shift of the species'

IR bands to lower frequencies—an observation that is inconsistent with the IR spectrum of the adsorbed species.

Insights into Thiophene Hydrodesulfurization over Sulfided Mo/Al_2O_3 Catalysts. When thiophene is η^1(S)-coordinated in $(\eta^5\text{-}C_5D_5)Re(CO)_2(\eta^1\text{(S)-}C_4H_4S)$, the $\nu(C{=}C)_{sym}$, $\nu(C{=}C)_{as}$, and "ν(C−C)" and ν(C−S) modes become shifted by +29, +31, and +10 cm^{-1} respectively, whereas the ν(C−S) band shifts by −123 cm^{-1} (i.e., in the opposite direction). As described earlier, the +22 cm^{-1} shift of the $\nu(C{=}C)_{sym}$ band of thiophene upon adsorption to cus Mo sites of sulfided Mo/Al_2O_3 catalysts is consistent with the shift observed for the thiophene ligand in $(\eta^5\text{-}C_5D_5)Re(CO)_2(\eta^1\text{(S)-}C_4H_4S)$. Close examination of the IR spectrum in Figure 6 for thiophene adsorbed on a sulfided Mo/Al_2O_3 catalyst does not reveal the expected shifts for the $\nu(C{=}C)_{as}$ and "ν(C−C)" bands. However, this observation is not surprising given the very weak intensity of the $\nu(C{=}C)_{as}$ band and the small shift expected for the "ν(C−C)" band. Unfortunately, the optical properties of γ-Al_2O_3 (IR cutoff at ∼950 cm^{-1}) do not allow for the observation of the thiophene adsorbate's ν(C−S) band, which is located at 751 cm^{-1} for gas-phase thiophene.

In addition to verifying our assignment of the adsorption mode of thiophene on sulfided Mo/Al_2O_3 catalysts, a key result of this study is the insight it provides into the thiophene HDS mechanism over these catalysts. Angelici,[8] Jones et al.,[60] and Bianchini and Meli[61] have recently reviewed the chemistry of thiophene coordinated to metal centers and its relationship to thiophene HDS, whereas Topsøe et al.[2] have summarized proposed reaction pathways for thiophene HDS over model catalysts.

As discussed above, the normal mode calculations of the IR spectra of η^1(S)-coordinated thiophene in $(\eta^5\text{-}C_5D_5)Re(CO)_2(\eta^1\text{(S)-}C_4H_4S)$ indicate that the carbon−carbon bonds in the C_4 hydrocarbon backbone are slightly strengthened while the carbon−sulfur bonds are substantially weakened relative to free thiophene. These bonding changes, and the definitive assignment of the adsorption mode of thiophene on sulfided Mo/Al_2O_3 catalysts to be η^1(S), suggest the initial steps in the thiophene HDS reaction to be the following: (1) η^1(S)-coordination of thiophene to a cus metal site, and (2) cleavage of one of the two weakened C−S bonds. This conclusion significantly narrows the number of possible reaction pathways by which thiophene HDS occurs on transition metal sulfide catalysts when considering mechanisms proposed in the organometallic and catalysis literatures. Focusing first on organometallic chemistry, reactivity has been observed for thiophene in different coordination geometries.[8] Indirect observations point to η^1(S)-coordinated thiophene being the immediate precursor to C−S bond cleavage in metal insertion reactions.[60,61] Chen et al.[62] have proposed a complete thiophene HDS mechanism in which the initial step is a C−S insertion by a metal atom (or ion); the initial hydrocarbon product of this mechanism is 1,3-butadiene.

On the basis of IR and TPD studies, Bussell and co-workers[4] concluded that C−S bond cleavage did not occur when a sulfided Mo/Al_2O_3 catalyst (14 wt % MoO_3) was annealed at 693 K in the presence of thiophene alone (P_{Th} = 9.5 Torr). However, when a sample of this same catalyst was annealed to 693 K in the presence of a thiophene/H_2 mixture (P_{Th} = 9.5 Torr, P_{H2} = 490.5 Torr), C−S bond cleavage to give a strongly adsorbed hydrocarbon fragment was observed. Subsequent temperature programmed desorption (TPD) in ultrahigh vacuum yielded desorption features for C_4 hydrocarbon (butadiene, butenes, and butane) and H_2S products.[4] Although there is no direct evidence to support this, the presence of H_2 may be required to reduce cus $Mo^{\delta+}$ species to a low enough oxidation state for the C−S insertion to occur. All of the known metal insertions into C−S bonds occur with metals in low oxidation states.[60]

Review of the catalysis literature points to the initial steps of the Lipsch and Schuit mechanism as being the most consistent with the observations of the cuurent study.[63] In this mechanism, thiophene adsorbs in an η^1(S)-geometry to a cus Mo site followed by successive cleavage of the C−S bonds to give 1,3-butadiene and an adsorbed sulfur atom. As discussed above, the results presented here indicate that the C−S bonds of thiophene η^1(S)-coordinated to cus Mo sites are significantly weakened, making them labile to cleavage. Once the first C−S bond is cleaved, the remaining adsorbed butadienethiolate species is no longer aromatic and would be expected to be quite reactive on a catalyst surface. This species would likely undergo further reaction much more quickly than the initial C−S bond cleavage and it is difficult to predict what would occur next.

Conclusions

Infrared spectra acquired for three organometallic complexes: $(\eta^5\text{-}C_4H_4S)Cr(CO)_3$, $[(\eta^5\text{-}C_4H_4S)Mn(CO)_3]BF_4$ and $(\eta^5\text{-}C_5D_5)Re(CO)_2(\eta^1\text{(S)-}C_4H_4S)$ were analyzed in detail. The spectral shift of the $\nu(C{=}C)_{sym}$ mode observed in the IR spectrum of the η^1(S)-coordinated thiophene ligand in $(\eta^5\text{-}C_5D_5)Re(CO)_2(\eta^1\text{(S)-}C_4H_4S)$, with respect to the IR spectrum of the free species, was similar in both magnitude and direction to that observed for the analogous band of thiophene adsorbed at the surface of a sulfided Mo/Al_2O_3 catalyst. Normal mode calculations were used to model the IR spectra of thiophene coordinated in $(\eta^5\text{-}C_4H_4S)Cr(CO)_3$ and $(\eta^5\text{-}C_5D_5)Re(CO)_2(\eta^1\text{(S)-}C_4H_4S)$. Perturbations among the force constants of a gas-phase thiophene model, consistent with molecular orbital and X-ray diffraction studies of η^1(S)- and η^5-coordinated thiophene ligands, gave rise to respective force fields that were in turn utilized to accurately model the IR spectra of thiophene coordinated in the Cr and Re complexes. Furthermore, perturbations among the force constants of the η^1(S)-coordinated thiophene model, necessary to emulate the observed spectral shifts, are consistent with a thiophene HDS mechanism that involves cleavage of one of the C−S bonds of η^1(S)-adsorbed thiophene in its initial step. Specifically, the IR spectrum of η^1(S)-coordinated thiophene, as recorded for the ligand in $(\eta^5\text{-}C_5D_5)Re(CO)_2(\eta^1\text{(S)-}C_4H_4S)$, can only be modeled through perturbation of the respective model's force constants consistent with a slight increase of electron density within the thiophene ligand's C=C−C=C fragment (11% and 5% for C=C and C−C bonds, respectively) and a concomitant depletion of electron density within the species' C−S coordinates (37%). Thus, it is concluded that thiophene adopts an η^1(S)-coordination at cus Mo sites of sulfided Mo/Al_2O_3 catalysts and that this species, in the presence of hydrogen, undergoes C−S bond cleavage. Studies are under way in order to further clarify the HDS reaction mechanism of the η^1(S)-coordinated thiophene on sulfided Mo/Al_2O_3 catalysts.

Acknowledgment. This research was supported by the National Science Foundation under grant number CHE-9610438 (M.E.B.) and by the U.S. Department of Energy, Office of Science, Office of Basic Energy Sciences, Chemical Sciences Division, under contract W-7450-Eng-82 with Iowa State University (R.J.A.). Acknowledgment is also made to the donors of the Petroleum Research Fund, administered by the ACS, and the Henry Dreyfus Teacher-Scholar Awards Program of the

Camille and Henry Dreyfus Foundation for partial support of this research (M.E.B.).

References and Notes

(1) Prins, R.; de Beer, V. H. J.; Somorjai, G. A. *Catal. Rev. Sci. Eng.* **1989**, *31*, 1.
(2) Topsøe, H.; Clausen, B.; Massoth, F. E. Hydrotreating Catalysis. In *Catalysis: Science and Technology*; Anderson, J. R., Boudart, M., Eds.; Springer-Verlag: Berlin, 1996; Vol. 11; p 1.
(3) Mitchell, P. C. H.; Green, D. A.; Payen, E.; Tomkinson, J.; Parker, S. F. *Phys. Chem. Chem. Phys.* **1999**, *1*, 3357.
(4) Tarbuck, T. L.; McCrea, K. M.; Logan, J. W.; Heiser, J. L.; Bussell, M. E. *J. Phys. Chem. B* **1998**, *102*, 7845.
(5) Mills, P.; Phillips, D. C.; Woodruff, B. P.; Main, R.; Bussell, M. E. *J. Phys. Chem. B* **2000**, *104*, 3237.
(6) Rauchfuss, T. B. *Prog. Inorg. Chem.* **1991**, *39*, 259.
(7) Angelici, R. J. *Bull. Soc. Chim. Belg.* **1995**, *104*, 265.
(8) Angelici, R. J. *Polyhedron* **1997**, *16*, 3073.
(9) Dong, L.; Duckett, S. B.; Ohman, K. F.; Jones, W. D. *J. Am. Chem. Soc.* **1992**, *114*, 151.
(10) Hachgenei, J. W.; Angelici, R. J. *J. Organomet. Chem.* **1988**, *355*, 359.
(11) Luo, S.; Rauchfuss, T. B.; Gan, Z. *J. Am. Chem. Soc.* **1993**, *115*, 4943.
(12) Chen, J.; Daniels, L. M.; Angelici, R. J. *J. Am. Chem. Soc.* **1990**, *112*, 199.
(13) Zaera, F. *Chem. Rev.* **1995**, *95*, 2651.
(14) Scott, D. W. *J. Mol. Spec.* **1969**, *31*, 451.
(15) Cyvin, B. N.; Cyvin, S. J. *Acta Chem. Scand.* **1969**, *23*, 3139.
(16) Orza, J. M.; Rico, M.; Biarge, F. *J. Mol. Spec.* **1966**, *19*, 188.
(17) Simandiras, E. D.; Handy, N. C.; Amos, R. D. *J. Phys. Chem.* **1988**, *92*, 1739.
(18) El-Azhary, A. A.; Hilal, R. H. *Spectrochim. Acta* **1997**, *53A*, 1365.
(19) El-Azhary, A. A.; Suter, H. U. *J. Phys. Chem.* **1996**, *100*, 15 056.
(20) Kwiatkowski, J. S.; Leszczynski, J.; Teca, I. *J. Mol. Struct.* **1997**, *436/437*, 451.
(21) Harris, S. *Organometallics* **1994**, *13*, 2628.
(22) Harris, S. *Polyhedron* **1997**, *16*, 3219.
(23) Rincón, L.; Terra, J.; Guenzburger, D.; Sánchez-Delgado, R. A. *Organometallics* **1995**, *14*, 1292.
(24) Sargent, A. L.; Titus, E. P.; Riordan, C. G.; Rheingold, A. L.; Ge, P. *Inorg. Chem.* **1996**, *35*, 7095.
(25) Sargent, A. L.; Titus, E. P. *Organometallics* **1998**, *17*, 65.
(26) Atter, G. D.; Chapman, D. M.; Hester, R. E.; Green, D. A.; Mitchell, P. C. H.; Tomkinson, J. *J. Chem. Soc., Faraday Trans.* **1997**, *93*, 2977.
(27) Rodriguez, J. A. *J. Phys. Chem. B* **1997**, *101*, 7524.
(28) Toulhoat, H.; Raybaud, P.; Kasztelan, S.; Kresse, G.; Hafner, J. *Catal. Today* **1999**, *50*, 629.
(29) Spies, G. H.; Angelici, R. J. *Organometallics* **1987**, *6*, 1897.
(30) Anderson, G. K.; Cross, R. J.; Phillips, I. G. *J. Chem. Soc., Chem. Commun.* **1978**, 709.
(31) Choi, M. G.; Angelici, R. J. *Organometallics* **1991**, *10*, 2436.
(32) Heah, P. C.; Patton, A. T.; Gladysz, J. A. *J. Am. Chem. Soc.* **1996**, *108*, 1185.
(33) Novi, M.; Guanti, G.; Dell'Erba, C. *J. Heterocycl. Chem.* **1975**, *12*, 1055.
(34) Gracey, D. E. F.; Jackson, W. R.; Jennings, W. B.; Mitchell, T. R. B. *J. Chem. Soc. B.* **1969**, 1204.
(35) Chen, J.; Young, V. G.; Angelici, R. J. *Organometallics* **1996**, *15*, 325.
(36) McIntosh, D. F.; Peterson, M. R. QCPE Program No. QCPE 067; Quantum Chemistry Program Exchange, Indiana University, Department of Chemistry:, 1988.
(37) Wilson, E. B.; Decius, J. C.; Cross, P. C. *Molecular Vibrations, The Theory of Infrared and Raman Vibrational Spectra*; Dover Publications: New York, 1980.
(38) Mills, P.; Jentz, D.; Trenary, M. *J. Mol. Catal.* **1998**, *131*, 209.
(39) Bak, B.; Christensen, D.; Hanse-Nygaard, L.; Rastrup-Andersen, J. *J. Mol. Spec.* **1961**, *7*, 58.
(40) Blom, C. E.; Altona, C. *Mol. Phys.* **1977**, *3*, 875.
(41) Wiberg, K. B.; Waddell, S. T.; Rosenburg, R. E. *J. Am. Chem. Soc.* **1990**, *112*, 1509.
(42) Hu, S.; Mukherjee, A.; Spiro, T. G. *J. Am. Chem. Soc.* **1993**, *115*, 12366.
(43) Dumbacker, B. *Theoretical Chimica Acta* **1972**, *23*, 346.
(44) Burgi, H. B.; Dunitz, J. D. *J. Am. Chem. Soc.* **1987**, *109*, 2924.
(45) Draganjac, M.; Ruffing, C. J.; Rauchfuss, T. B. *Organometallics* **1985**, *4*, 1909.
(46) Benson, J. W.; Angelici, R. J. *Organometallics* **1992**, *11*, 922.
(47) Sanger, M. J.; Angelici, R. J. *Organometallics* **1994**, *13*, 1821.
(48) Polam, J. R.; Porter, L. C. *Organometallics* **1993**, *12*, 3504.
(49) Sánchez-Delgado, R. A.; Marquez-Silva, R. L.; Puga, J.; Tiripicchio, A.; Tiripicchio, C. *J. Organomet. Chem.* **1986**, *316*, C35.
(50) Butler, I. S.; Li, H.; Gao, J. P. *Appl. Spec.* **1991**, *45*, 223.
(51) Lokshin, B. V.; Rusach, E. B.; Konovalov, T. D. *Izv. Akad. Nauk SSSR, Ser. Khim.* **1975**, 84.
(52) Chhor, K.; Lucazeau, G. *Spectrochim. Acta* **1982**, *38A*, 1163.
(53) Maslowsky, E. J. *Vibrational Spectra of Organometallic Compounds*; John Wiley and Sons: New York, 1977.
(54) Rico, M.; Orza, J. M.; Morcillo, J. *Spectrochim. Acta* **1965**, *21*, 689.
(55) Mills, P.; Jentz, D.; Celio, H.; Trenary, M. *J. Am. Chem. Soc.* **1996**, *118*, 6524.
(56) Müller, B.; Langeveld, A. D. v.; Moulijn, J. A.; Knözinger, H. *J. Phys. Chem.* **1993**, *97*, 9028.
(57) Quigley, W. W. C.; Yamamoto, H. D.; Aegerter, P. A.; Simpson, G. J.; Bussell, M. E. *Langmuir* **1996**, *12*, 1500.
(58) Kline, C. H.; Turkevich, J. *J. Chem. Phys.* **1944**, *12*, 300.
(59) Kiviat, F. E.; Petrakis, L. *J. Phys. Chem.* **1973**, *77*, 1232.
(60) Jones, W. D.; Vicic, D. A.; Chin, R. M.; Roache, J. H.; Myers, A. W. *Polyhedron* **1997**, *16*, 3115.
(61) Bianchini, C.; Meli, A. *Acc. Chem. Res.* **1998**, *31*, 109.
(62) Chen, J.; Daniels, L. M.; Angelici, R. J. *J. Am. Chem. Soc.* **1991**, *113*, 2544.
(63) Lipsch, J. M. J. G.; Schuit, G. C. A. *J. Catal.* **1969**, *15*, 179.